Symmetrical and Unsymmetrical Quadruply Aza Bridged Closely Interspaced Cofacial Bis(5,10,15,20-tetraphenylporphyrin)s. 2. Synthesis, Characterization, and Conformational Effects of Solvents

Rafik Karaman, Andrei Blaskó, Örn Almarsson, Ramesh Arasasingham, and Thomas C. Bruice*

Contribution from the Department of Chemistry, University of California at Santa Barbara, Santa Barbara, California 93106. *Received November 4, 1991*

Abstract: Several water- and non-water-soluble symmetrical and unsymmetrical quadruply aza bridged closely interspaced cofacial bis(5,10,15,20-tetraphenylporphyrin)s have been synthesized and fully characterized by 2D ^1H–^1H NMR (COSY), 2D ^{13}C–^1H NMR, FABMS, UV/vis, IR, and fluorescence spectral techniques. It was established, on the basis of ^1H NMR, UV/vis, and emission spectrophotometries, that tetrakis[*m*,*m*-(methylene(*m*-pyridinesulfonyl)imino)methylene]-strati-bis-(5,10,15,20-tetraphenylporphyrin) (**5**), tetrakis[*m*,*m*-(methylene(*m*-pyridiniumsulfonyl)imino)methylene]-strati-bis-(5,10,15,20-tetraphenylporphyrin) chloride (**7**), and tetrakis[*m*,*m*-(methylene(*p*-toluenesulfonyl)imino)methylene]-strati-bis(5,10,15,20-tetraphenylporphyrin) (**11**) exist in more than one conformation in DMSO and in only one symmetrical conformation in $CHCl_3$. The biszinc and tetraprotonated **5**, **7**, and **11** exist in one conformation regardless of the solvent. These observations have been attributed to an interaction between DMSO and the pyrrolic N–H protons of the porphyrin cores which is inhibited by metalation (Zn^{2+}) or protonation of the porphyrin moiety. Molecular dynamics calculations reveal that the intracavity interactions of **5** with DMSO are more important than the intercavity interactions which result in discrete, unsymmetrical conformations of the dimer. In contrast, tris[*m*,*m*-(methylene(*m*-pyridinesulfonyl)imino)methylene]-mono((((methyleneoxy)carbonyl)oxy)methylene)-strati-bis(5,10,15,20-tetraphenylporphyrin) (**6**), tetrakis[*m*,*m*-(methylenecyanoimino)-methylene]-strati-bis(5,10,15,20-tetraphenylporphyrin) (**8**), tris[*m*,*m*-(methylenecyanoimino)methylene]-mono((((methyleneoxy)carbonyl)oxy)methylene)-strati-bis(5,10,15,20-tetraphenylporphyrin) (**9**), and tetrakis[*m*,*m*-(methylene(formamido)imino)methylene]-strati-bis(5,10,15,20-tetraphenylporphyrin) (**10**) do not show any conformational changes upon switching from chloroform to DMSO. This is attributed to the long interplanar distances calculated for the porphyrin dimers which prevent any intracavity coordination of DMSO with both porphyrin moieties. ^1H NMR variable-temperature experiments of porphyrin dimer **5** in DMSO show that the conformation of the dimer is greatly affected by temperature. While at room temperature **5** exists in more than one conformation, at higher temperatures (150 °C) only one conformation is populated. It is proposed that at room temperature, the existence of a hydrogen-bonding network between DMSO and the dimer results in more than one conformation, while at higher temperatures the network is destroyed to furnish an average conformation.

Introduction

Covalently linked metalloporphyrin dimers have attracted considerable interest among chemists[1] as models for metalloenzymes such as cytochrome c_3,[2] cytochrome *c* oxidase,[3] superoxide dismutase,[4] nitrogenase,[5] and others[6] because they provide a means of bringing into proximity and orienting ligated metal centers.[7] Binding of oxygen and carbon monoxide to imidazole complexes of copper–iron porphyrin dimers has been studied, and it has been shown that the lifetime of the oxygen binding is long and that of the latter is much reduced.[8] Furthermore, cofacial dimeric, trimeric, and pentameric porphyrins have been studied as pho-

Chart I

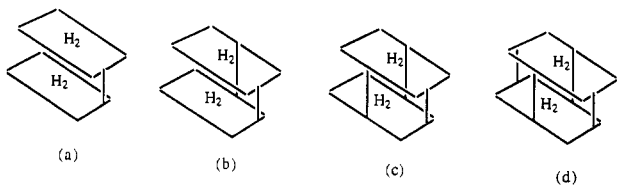

(a), (b), (c) and (d) are singly-, doubly-, triply-, and quadruply-bridged cofacial dimeric porphyrins, respectively.

(1) For a review of the literature up to 1980, see: Dolphin, D.; Hiom, J.; Paine, J. B., III. *Heterocycles* **1981**, *16*, 417.
(2) Yagi, T.; Aruyama, K. *Biochim. Biophys. Acta* **1971**, *243*, 214.
(3) (a) Hatada, M. H.; Tulinsky, A.; Chang, C. K. *J. Am. Chem. Soc.* **1980**, *102*, 7115. (b) Collman, J. P.; Anson, F. C.; Barnes, C. E.; Bencosme, C. S.; Geiger, T.; Evitt, E. R.; Kreh, R. P.; Meier, K.; Pettman, R. B. *J. Am. Chem. Soc.* **1983**, *105*, 2694. (c) Durand, R. R., Jr.; Bencosme, C. S.; Collman, J. P.; Anson, F. C. *Ibid.* **1983**, *105*, 2710. (d) Le Mest, Y.; L'Her, M.; Courtot-Coupez, J.; Collman, J. P.; Evitt, E. R.; Bencosme, C. S. *J. Chem. Soc., Chem. Commun.* **1983**, 1286. (e) Chang, C. K.; Liu, H. Y.; Abdalmuhdi, I. *J. Am. Chem. Soc.* **1984**, *106*, 2725. (f) Filler, J. P.; Ravichandran, K. G.; Abdalmuhdi, I.; Tulinsky, A.; Chang, C. K. *J. Am. Chem. Soc.* **1986**, *108*, 417. (g) Le Mest, Y.; L'Her, M.; Collman, J. P.; Hendricks, N. H.; McElwee-White, L. *J. Am. Chem. Soc.* **1986**, *108*, 533. (h) Collman, J. P.; Kim, K. *Ibid.* **1986**, *108*, 7847. (i) Collman, J. P.; Hendricks, N. H.; Kim, K.; Bencosme, C. S. *J. Chem. Soc., Chem. Commun.* **1987**, 1537. (j) Kim, K.; Collman, J. P.; Ibers, J. A. *J. Am. Chem. Soc.* **1988**, *110*, 4242. (k) Proniewicz, L. M.; Odo, J.; Goral, J.; Chang, C. K.; Nakamoto, K. *J. Am. Chem. Soc.* **1989**, *111*, 2105.
(4) (a) Landrum, J. T.; Reed, C. A.; Hatano, K.; Scheidt, W. R. *J. Am. Chem. Soc.* **1978**, *100*, 3232. (b) Landrum, J. T.; Grimmett, D.; Haller, K. J.; Scheidt, W. R.; Reed, C. A. *J. Am. Chem. Soc.* **1981**, *103*, 2640.
(5) (a) Winter, H. C.; Burris, R. H. *Annu. Rev. Biochem.* **1976**, *45*, 409. (b) Shah, V. K.; Brill, W. J. *Proc. Natl. Acad. Sci. U.S.A.* **1979**, *74*, 3249.
(6) Cohen, I. A. *Struct. Bonding* **1980**, *40*, 1.
(7) Collman, J. P.; Anson, F. C.; Bencosme, S.; Chong, A.; Collins, T.; Denisevich, P.; Evitt, E.; Geiger, T.; Ibers, J. A.; Jameson, G.; Konai, Y.; Koval, C.; Meier, K.; Okaley, P.; Pettman, R.; Schmittou, E.; Sessler, J. In *Organic Synthesis Today and Tomorrow*; Trost, B. M., Hutchinson, C. R., Eds.; Pergamon Press: Oxford, 1981; pp 29–45.
(8) (a) Chang, C. K. *ACS Adv. Chem. Ser.* **1979**, *173*, 162. (b) Ward, B.; Wang, C. B.; Chang, C. K. *J. Am. Chem. Soc.* **1981**, *103*, 5236. (c) Tsuchida, E.; Nishide, H. "Hemoglobin Model-Artifical Oxygen Carrier Composed of Porphinatoiron Complexes." *Top. Curr. Chem.* **1986**, *128*, 63.

0002-7863/92/1514-4889$03.00/0

tooxidation devices of water to mimic the photosynthetic photocatalytic oxidization of water to dioxygen.[1,9] Stacked dimeric metalloporphyrins have been examined for their electrical conductivities, and it has been suggested that these species could be used in the development of electronic devices.[10] Metalloporphyrins with large cavities have been designed and assembled with the idea of creating multisite complexing hosts incorporating functionalized subunits for binding organic substrates and transition metals so as to mimic metalloenzymes, as well as supermolecular photochemical devices.[11]

Covalently linked cofacial tetraphenylporphyrin dimers may be singly, doubly, triply, or quadruply bridged (Chart I). The structural flexibility of the dimeric porphyrin is largely determined by the number and the nature of the bridges, and the size of the cavity and the interplanar distance between the two porphyrin cores are determined by the length of the bridges.[12] We have recently become interested in the chemistry of quadruply bridged–cofacial dimeric porphyrins. There existed only one such compound[13] prior to our recent report of procedures for the general preparation of quadruply bridged closely interspaced porphyrin dimers based upon structure A.[14] We now report the synthesis, the characterization and the physical properties of some representatives of water- and non-water-soluble symmetrical and unsymmetrical quadruply aza bridged closely interspaced cofacial bis(5,10,15,20-tetraphenylporphyrin)s.

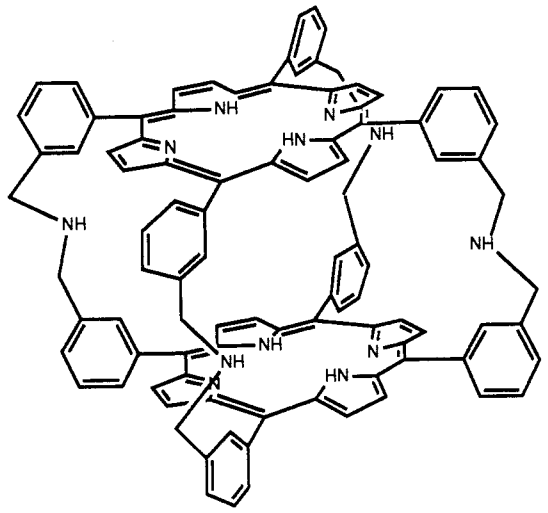

Structure A

(9) (a) Wasielewski, M. R.; Svec, W. A.; Cope, B. T. *J. Am. Chem. Soc.* **1978**, *100*, 1962. (b) Boxer, S. G.; Closs, G. L. *J. Am. Chem. Soc.* **1976**, *98*, 340. (c) Bucks, R. R.; Boxer, S. G. *J. Am. Chem. Soc.* **1982**, *104*, 340. (d) Netzel, T. L.; Bergkamp, M. A.; Chang, C. K. *J. Am. Chem. Soc.* **1982**, *104*, 1952.

(10) (a) Cowan, J. A. *J. Chem. Soc., Dalton Trans.* **1988**, 2681. (b) Hunter, C. A.; Leighton, P.; Sanders, J. K. M. *J. Chem. Soc., Perkin Trans. 1* **1989**, 547. (c) Hunter, C. A.; Sanders, J. K. M. *J. Am. Chem. Soc.* **1990**, *112*, 5525. (d) Naylor, S.; Hunter, C. A.; Cowan, J. A.; Lamb, J. H.; Sanders, J. K. M. *J. Am. Chem. Soc.* **1990**, *112*, 6507.

(11) (a) Hamilton, A. D.; Lehn, J.-M.; Sessler, J. L. *J. Chem. Soc., Chem. Commun.* **1984**, 311. (b) Dubowchik, G. M.; Hamilton, A. D. *J. Chem. Soc., Chem. Commun.* **1985**, 904. (c) Dubowchik, G. M.; Hamilton, A. D. *J. Chem. Soc., Chem. Commun.* **1987**, 293. (d) Hunter, C. A.; Meah, M. N.; Sanders, J. K. M. *J. Chem. Soc., Chem. Commun.* **1988**, 692.

(12) (a) Collman, J. P.; Marrocco, M.; Denisevich, P.; Koval, C.; Anson, F. C. *J. Electroanal. Chem.* **1979**, *101*, 117. (b) Collman, J. P.; Denisevich, P.; Konai, Y.; Marrocco, M.; Koval, C.; Anson, F. C. *J. Am. Chem. Soc.* **1980**, *102*, 6027. (c) Geiger, T.; Anson, F. C. *J. Am. Chem. Soc.* **1981**, *103*, 7489. (d) Liu, H. Y.; Abdalmuhdi, I.; Chang, C. K.; Anson, F. C. *J. Phys. Chem.* **1985**, *89*, 665. (e) Liu, H. Y.; Weaver, M. J.; Wang, C.-B.; Chang, C. K. *J. Electroanal. Chem.* **1983**, *145*, 439. (f) Sawaguchi, T.; Matsue, T.; Itaya, K.; Uchida, I. *Electrochim. Acta* **1991**, *36*, 703. (g) Collman, J. P.; Hendricks, N. H.; Leidner, C. R.; Ngameni, E.; L'Her, M. *Inorg. Chem.* **1988**, *27*, 387. See also ref 3c, 3e, and 7.

(13) (a) Kagan, N. E.; Mauzerall, D.; Merrifield, R. B. *J. Am. Chem. Soc.* **1977**, *99*, 5484. (b) Kagan, N. E. In *Porphyrin Chemistry Advances*; Longo, F. R., Ed.; Ann Arbor Science: Ann Arbor, MI, 1979; pp 43–50.

(14) Bookser, B. C.; Bruice, T. C. *J. Am. Chem. Soc.* **1991**, *113*, 4208.

Results and Discussion

The modeling studies of metalloenzymes utilizing closely interspaced porphyrin dimers have been restricted to organic solvents due to the insolubility of the dimers in aqueous media. It is of great importance to design model compounds that are water soluble. This could be achieved by introducing hydrophilic groups or/and negative or positive charges on the model compound. With this in mind, we have designed two quadruply bridged closely interspaced porphyrin dimers (**7** and **12**) that fulfill this requirement. In addition, porphyrins **7** and **12** incorporate the following features: (1) aryl substitution on all meso carbons of the porphyrin cores to prevent unwanted oxidation of the porphyrin moieties; (2) hydrophilic and lipophilic groups to assist the membrane penetration properties of the species; (3) four cationic groups to enable anionic species to be attracted to the cavity of the porphyrin cores; (4) a relatively small cavity with the appropriate geometrical disposition so as to have the required binding properties for small molecules such as dioxygen.

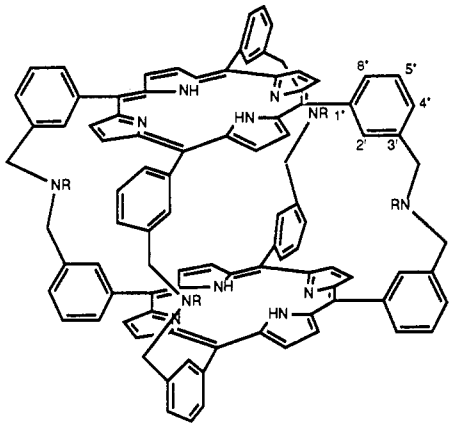

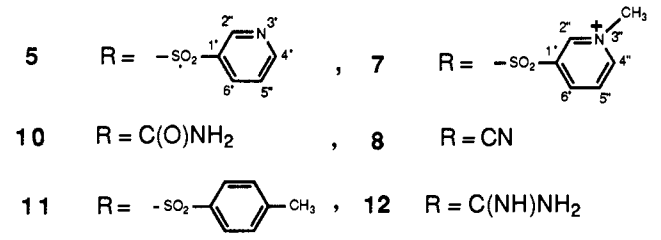

5 R = , **7** R =

10 R = $C(O)NH_2$, **8** R = CN

11 R = , **12** R = $C(NH)NH_2$

14 R = C(NH)OEt

Synthesis. 5,10,15,20-Tetrakis(α-bromo-*m*-tolyl)porphyrin (**2**) has been synthesized from α-bromo-*m*-toluenaldehyde (**1**) by modification of previous procedures.[14] Compounds **1**[15] and **2**[14,16]

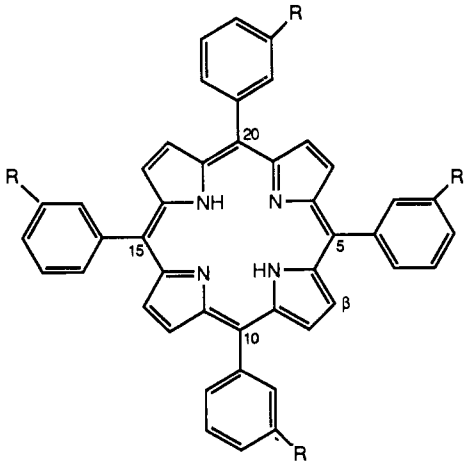

2 $R = CH_2Br$

13 R = CN

were obtained in 84% and 24% yields, respectively. Reaction of 3-pyridinesulfonic acid with excess phosphorus pentachloride in the presence of phosphorus oxychloride (120 °C, 12 h) provided 3-pyridinesulfonyl chloride (**3**) in 98% yield.[17] Reaction of **3** with 28% aqueous ammonium hydroxide solution (50 °C, 2 h) followed by selective solubilization and crystallization afforded 3-pyridinesulfonamide (**4**) in 69% yield.[18]

Following the self-assembly procedure[14] involving base-mediated (Cs_2CO_3) high-dilution coupling of 2 equiv of **2** with 4 equiv of pyridinesulfonamide or cyanamide in DMF and isolation by chromatography on silica gel using mixtures of chloroform/methanol as eluents afforded the symmetrical quadruply bridged closely interspaced porphyrin dimers tetrakis[*m*,*m*-(methylene-(*m*-pyridinesulfonyl)imino)methylene]-strati-bis(5,10,15,20-tetraphenylporphyrin) (**5**)[16] and tetrakis[*m*,*m*-(methylene(cyanimino)methylene]-strati-bis(5,10,15,20-tetraphenylporphyrin) (**8**)[14] in 12% and 5% yields, respectively. In addition, the unsymmetrical dimers, tris[*m*,*m*-(methylene(*m*-pyridinesulfonyl)imino)-methylene]-mono((((methyleneoxy)carbonyl)oxy)methylene)-strati-bis(5,10,15,20-tetraphenylporphyrin) (**6**), and tris[*m*,*m*-(methylenecyanimino)methylene]-mono((((methyleneoxy)-carbonyl)oxy)methylene)-strati-bis(5,10,15,20-tetraphenyl-porphyrin) (**9**) were isolated in 1.2% and 1% yields, respectively

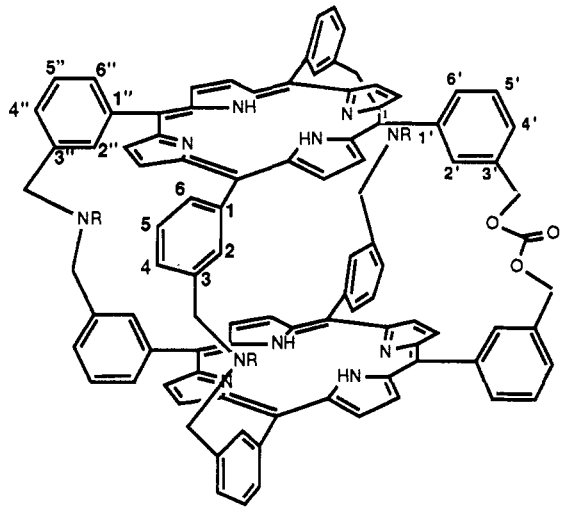

6 R = 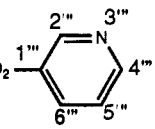 , **9** R = CN

(see Schemes I and II). When the coupling reaction was carried out using 2 equiv of **2** and only 3 equiv of either pyridinesulfonamide or cyanamide, the unsymmetrical dimers **6** and **9** were obtained in 3.4% and 3% yields, respectively, along with the formation of the symmetrical dimers **5** and **8** in 7% and 4% yields, respectively. The mechanism by which the symmetrical dimers **5** and **8** are formed is illustrated in Scheme I. In the first step, the substituted amide (cyanamide or pyridinesulfonamide) undergoes deprotonation to furnish the corresponding amidic salt I, which in a later step attacks the four electrophilic centers of **2** to form intermediate II, which finally, upon ionization followed by nucleophilic attack on **2**, provides the dimeric products. Proof for the intermediacy of II is provided by the formation of **5** from the basic catalyzed coupling reaction of intermediate II, synthesized independently, with **2**. The formation of the unsymmetrical dimers **6** and **9** is understood by the mechanism depicted in Scheme II, which involves nucleophilic attack of the amidic

Scheme I

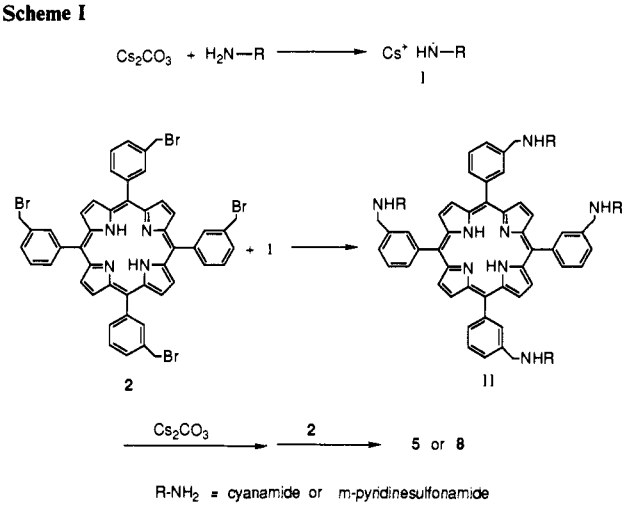

Scheme II

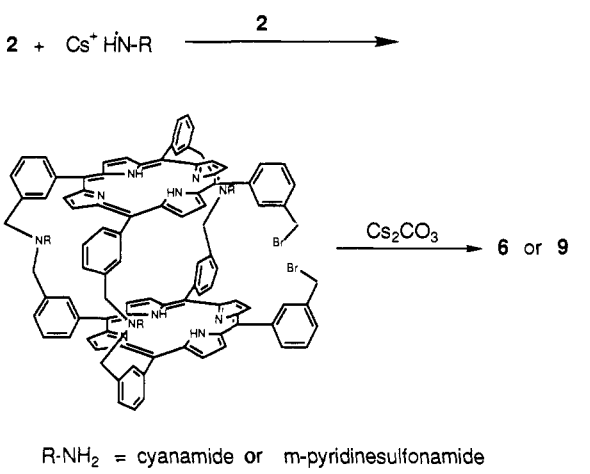

salt I on only three benzylic positions of **2** followed by condensation of the resulting intermediate with another molecule of **2** to give IV, which finally, upon nucleophilic attack of Cs_2CO_3 on its two benzylic centers, provides products. In Scheme I, Cs_2CO_3 behaves as a base, whereas in Scheme II it behaves as a base and as a nucleophile. The formation of the unsymmetrical dimers **6** and **9** as minor products is attributed to the lower nucleophilicity of Cs_2CO_3 compared to that of the amidic salts.

The water-soluble tetracationic quadruply bridged closely interspaced porphyrin dimer **7** was prepared in 70% yield from the alkylation reaction of a chloroform/acetone solution of **5** with excess methyl iodide (reflux, overnight) followed by separation on a reverse-phase TLC plate using acetone/water/NaCl as an eluent. The corresponding chloride salt was obtained by ion-exchange resin in the chloride form (Dowex IX8-100/Cl^-). Attempts to carry out the alkylation of **5** with methyl *p*-toluenesulfonate failed to give the desired product, and instead, N-alkylation on the pyrrolic rings occurred as judged by the UV/vis and ^1H NMR of the reaction mixture. Reaction of **8** with an ethanolic solution of trifluoroacetic acid (reflux, 72 h) and subsequent ammonolysis of the resultant imine **14** failed to give the water-soluble tetraguanidino dimer **12**, and instead, it afforded tetrakis[*m*,*m*-(methylene(formamido)imino)methylene]-strati-bis(5,10,15,20-tetraphenylporphyrin), **10**, in 76% yield (see Scheme III). The formation of **10** is presumably due to the presence of moisture in the reaction mixture. Attempts to conduct the reaction under very dry conditions failed to give **12**, but instead, dimer **10** was obtained. This may be due to the fact that the starting quantities of porphyrin **8** are low and subsequently very tiny amounts of water will lead to the hydrolysis of imine **14** to dimer **10**.

The biszinc porphyrin dimers Zn_2-**5** and Zn_2-**7** were obtained in good yields from the reactions of the corresponding porphyrin

(15) Sun, Y.; Martell, A. E.; Chen, D.; Macfarlane, R. D.; McNeal, C. J. *J. Heterocycl. Chem.* **1986**, *23*, 1565.
(16) Karaman, R.; Bruice, T. C. *J. Org. Chem.* **1991**, *56*, 3470.
(17) Franklin, J. *Inst.* **1943**, *236*, 316–320; *Chem. Abstr.* **1943**, *37*, 6652.
(18) Machek, G. *Monatsh. Chem.* **1938**, *72*, 77–92; *Chem. Abstr.* **1938**, *32*, 9087.

Scheme III

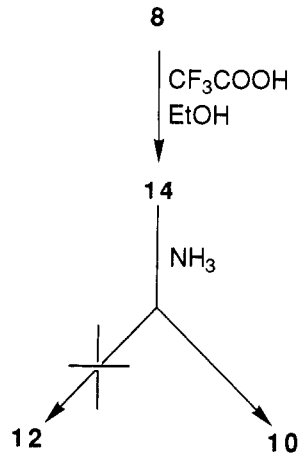

Table I. NMR Parameters of Porphyrin Dimers **5** and **9** at 25 °C in $CDCl_3$

5			9		
atom	δ_H, ppm (J, Hz)	δ_C, ppm	atom	δ_H, ppm (J, Hz)	δ_C, ppm
1′		141.96	1		142.40
2′	7.059	135.06	2	7.217	134.44
3′		132.57	3		132.45
4′	7.760 (d, 6.5)	128.58	4	7.849 (d, 7.5)	128.45
5′	7.627 (t, 7.5)	127.42	5	7.760 (t, 7.5)	127.52
6′	7.963 (d, 6.5)	133.21	6	8.217 (d, 7.0)	133.75
1″		137.98	1′		142.16
2″	9.230	148.23	2′	8.005	134.24
4″	8.885 (d, 6.0)	153.17	3′		131.46
5″	7.559 (t, 8.5)	123.66	4′	7.492 (d, 7.5)	126.28
6″	8.288 (d, 8.0)	134.90	5′	7.523 (t, 7.5)	125.51
CH_2	4.691	49.50	6′	7.972 (d, 7.0)	133.40
α-pyr		143.3[a]	1″		142.40
β-pyr	8.160	130.69	2″	7.687	134.57
meso		118.31	3″		132.45
NH	−4.34		4″	7.879 (d, 8.0)	128.45
			5″	7.714 (t, 7.5)	127.52
			6″	8.217 (d, 7.0)	133.75
			CH_2	4.334	54.10
			CH_2'	5.495	68.88
			CH_2''	4.513	54.19
			C(O)		170.40
			CN		118.20
			CN″		119.40
			α-pyr		149.34
			β,β″-pyr	8.434	130.86[b]
			β′-pyr	8.402	130.86[b]
			meso		118.51
			NH	−3.750	

[a] $\nu_{1/2}$ = 250 Hz. [b] $\nu_{1/2}$ = 800–1000 Hz.

dimers with zinc acetate (or chloride).

Characterization. Porphyrin dimers **5–10** were characterized by IR, UV/vis, fluorescence, FABMS, and NMR (1D ^1H, ^{13}C, 2D ^1H–^1H double quantum shift correlation, and ^{13}C–^1H J-correlated spectroscopies) spectroscopic methods.

Porphyrin Dimer 5. The IR spectrum of **5** shows a weak absorbance at 3320 cm^{-1} corresponding to pyrrolic N–H, two medium absorbances at 1600 and 1575 cm^{-1} corresponding to C=C and C=N, respectively, and strong bands at 1160 and 1110 cm^{-1} corresponding to SO_2. FABMS shows a molecular peak M^+ at 1956.6 and a peak at 1814.6 corresponding to $M^+ - C_5H_4N_2O_2S$. Assignments of the ^1H NMR resonances of **5** were based on the phase-sensitive double-quantum-filtered COSY experiment (DQF-COSY) (Table I). Interesting observations recorded in Table I follow. The ^1H NMR spectrum of **5** exhibits a resonance at −4.31 ppm corresponding to pyrrolic NH protons, a resonance at 4.66 ppm corresponding to the benzylic protons (CH_2), a resonance at 8.16 ppm corresponding to β-pyrrolic protons, and

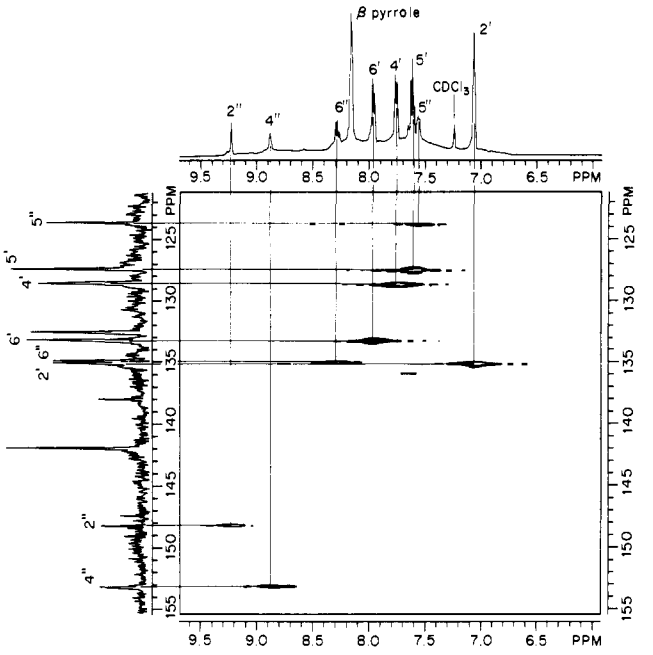

Figure 1. 2D ^{13}C–^1H correlation NMR spectrum of **5** in $CDCl_3$.

resonances in the region of 7.0–9.1 ppm corresponding to the phenylic and pyridinic protons (Table I). An interesting feature is the upfield shift of the $H_{2'}$ resonance (7.06 ppm) and downfield shifting of the $H_{6'}$ resonance (7.96 ppm). The shielding of the ortho-phenylic protons is due to the fact that $H_{2'}$ protons are pointing inside the shielding cone of the porphyrin core, and the deshielding of the $H_{6'}$ resonance is a result of $H_{6'}$ protons being outside the magnetic field of the porphyrin moieties. The ^{13}C NMR resonances were assigned according to both the 2D ^{13}C–^1H chemical shift correlation (Figure 1) and previous assignments of similar porphyrins[19] (Table I). The α-pyrrolic and the β-pyrrolic carbons appear at 143.3 ppm and at 130.7 ppm ($\nu_{1/2}$ = 250 Hz), respectively. The meso quaternary carbons resonate at 118.3 ppm, in the expected chemical shift range for that of tetraphenylporphyrin derivatives.[20] Assignments of C-1′ and C-1″ resonances (141.96 and 137.98 ppm, respectively) were based on calculations and relative intensities, and the remaining quaternary ^{13}C NMR resonance at 132.6 ppm was assigned for C-3′.

Porphyrin Dimer 6. The IR spectrum of **6** exhibits absorbances in the region of 3200 (w), 1740 (s), 1670 (m), and 1600 (m) cm^{-1} corresponding to pyrrolic NH, C=O, C=N, and C=C, respectively. FABMS shows two peaks, one at 1860.6 corresponding to M^+ and the other at 1718.6 corresponding to $M^+ - C_5H_4N_2O_2S$. Assignments of the ^1H and ^{13}C NMR resonances (see Experimental Section) were based on that of dimers **5** and **9**. The ^1H NMR spectrum shows a pyrrolic N–H resonance at −3.95 ppm, three benzylic resonances at 4.57, 4.75, and 5.42 ppm corresponding to CH_2, $CH_{2''}$ and $CH_{2'}$ (see structure), β-pyrrolic resonance at 8.18 ppm, and two sets of $H_{2'''}$ pyridinic protons in the region of 9.0–9.2 ppm (see Experimental Section). In the ^{13}C NMR spectrum, the meso carbons resonate at 118.3 ppm, the α-pyrrolic carbons appear at 142.1 ppm, the β-pyrrolic carbons resonate as a broad signal at 130.54 ppm, and the carbonyl carbons appear as a weak signal at 171.9 ppm.

Porphyrin Dimer 7. FABMS shows a base peak at 2017 corresponding to M^+ and a peak at 2002 corresponding to the $M^+ - CH_3$ fragment. The ^1H NMR spectrum in DMSO-d_6 shows four pyrrolic N–H resonances in the region of −5.2 to −6.1 ppm, two N-methyl and two benzylic resonances in the region of 4.8–5.7 ppm, and a complex aromatic region from 7.0 to 10.0 ppm. Upon heating the ^1H NMR sample at 150 °C, the N–H resonances in

(19) Garcia, B.; Lee, C.-H.; Blaskó, A.; Bruice, T. C. *J. Am. Chem. Soc.* **1991**, *113*, 8118.
(20) Abraham, R. J.; Hawkes, G. E.; Smith, K. M. *Tetrahedron Lett.* **1974**, *16*, 1483.

Table II. UV/Vis Spectra of Dimers and Monomers in DMSO and $CHCl_3$

compd	solvent	Soret band width at half peak height, nm	UV/vis λ_{max}, nm ($\epsilon \times 10^{-3}$ cm^{-1} M^{-1})
2	$CHCl_3$	12	419 (324), 515 (16.1), 549 (7.2), 589 (5.5), 646 (3.4)
2	DMSO	12	419 (315), 516 (15.9), 549 (7.2), 590 (5.5), 646 (3.4)
13	$CHCl_3$	12	419 (500), 514 (21.9), 548 (6.5), 589 (6.2), 644 (2.1)
13	DMSO	12	419 (520), 514 (25.1), 547 (5.7), 587 (5.5), 645 (2.0)
5	$CHCl_3$	19	414 (415), 514 (23.6), 550 (11.2), 591 (7.1), 647 (3.7)
5	DMSO	21	408 (463), 518 (15.8), 561 (9.6), 598 (4.4), 654 (3.0)
11	$CHCl_3$	19	414 (447), 515 (22.3), 550 (9.3), 591 (7.5), 647 (5.7)
11	DMSO	20	407 (520), 520 (18.1), 558 (9.9), 597 (4.7), 655 (3.8)
6	$CHCl_3$	19	416 (744), 517 (28.8), 553 (14.0), 591 (11.5), 648 (6.7)
6	DMSO	21	416 (636), 517 (36.1), 554 (13.3), 593 (9.0), 549 (7.2)
8	$CHCl_3$	18	415 (454), 514 (20.5), 550 (9.87), 591 (7.53), 649 (5.67)
8	DMSO	18	416 (462), 514 (20.8), 550 (10.9), 592 (8.25), 649 (6.2)
9	$CHCl_3$	17	416 (718), 516 (30.0), 551 (17.8), 593 (11.3), 647 (7.1)
9	DMSO	16	416 (667), 516 (28.2), 551 (14.7), 593 (9.5), 647 (6.6)

Table III. Emission Spectra of Dimers and Monomers in DMSO and $CHCl_3$

	emission spectra					
	rel intensity in $CHCl_3$		at λ^a		at λ^b	
compd	at λ^a	at λ^b	intensity ratio DMSO/$CHCl_3$	$\Delta\lambda$ (DMSO − $CHCl_3$)	intensity ratio DMSO/$CHCl_3$	$\Delta\lambda$ (DMSO − $CHCl_3$)
5	0.33	0.25	0.815	4.3	0.667	5.3
8	0.45	0.32	1.389	−0.5	1.155	0.5
9	1.0	0.76	1.355	0.0	1.125	0.0
11	0.24	0.17	1.069	5.3	0.866	4.8
13	1.0	1.0	1.954	−2.4	1.600	−2.0

[a] Around 650 nm. [b] Around 712 nm. For exact values of λ, see Experimental Section.

the region of −5.2 to −6.1 ppm coalesced to give only one resonance at −5.8 ppm. The ^1H NMR spectrum of tetraprotonated **7** in acetone-d_6 is more easily assignable. It shows a resonance at −4.3 ppm corresponding to pyrrolic NH, a broad resonance at 5.0 ppm corresponding to the benzylic and *N*-methylic protons, four phenylic resonances at 7.1, 7.9, 8.0, and 8.2 ppm, one β-pyrrolic resonance at 8.25 ppm, and four signals at 8.75, 9.4, 9.7, and 10.1 ppm corresponding to the pyridinic protons. The ^1H NMR spectrum of the biszinc complex of **7** in acetone-d_6 shows a broad resonance at 4.94 ppm corresponding to the benzylic and *N*-methyl protons, four phenylic resonances at 7.35, 7.78, 7.88, and 8.10 ppm, one β-pyrrolic resonance at 8.21 ppm, and four pyridinic resonances at 8.73, 9.39, 9.55, and 9.95 ppm. When the spectrum was taken in DMSO-d_6, the resonance at 4.94 ppm appears as two singlets: at 4.82 ppm corresponding to the benzylic protons and at 4.95 ppm corresponding to the *N*-methylic protons.

Porphyrin Dimer 8. This dimer was previously characterized by IR, FABMS, and ^1H NMR spectroscopic methods.[14] To fully characterize it, the ^{13}C NMR spectrum was taken in $CDCl_3$. It shows a resonance at 118.2 ppm corresponding to CN, a signal at 118.6 ppm corresponding to meso carbons, a broad peak for β-pyrrolic carbons at 130.8 ppm, and α-pyrrolic carbons resonating at 149.2 ppm (for full assignment, see Experimental Section).

Porphyrin Dimer 9. The IR spectrum shows absorbances at 3200 (w), 2210 (s), 1730 (s), and 1600 (m) cm^{-1} corresponding to pyrrolic NH, CN, C=O, and C=C, respectively. FABMS shows a peak at 1513 corresponding to M^+. The ^1H NMR spectrum shows a NH resonance at −3.75 ppm, three different sets of CH_2 signals, one at 5.49 ppm ($CH_{2'}$) corresponding to the benzylic protons of the carbonate linker and the other two at 4.33 (CH_2) and 4.51 ppm ($CH_{2''}$) corresponding to the unidentical cyanamide linkers (see Table I and Figure 2), and two signals of β-pyrrolic protons appearing at 8.43 (β,β'') and 8.402 ppm (β') (ratio 3:1). The small β-pyrrolic signal (10–15% of β') at 8.52 ppm is due to a partial protonation of the porphyrin by a trace amount of acid in the solvent ($CDCl_3$). Assignments of the ^{13}C NMR resonances (Table I) were based on those for dimers **5** and **8**. The low-intensity α-pyrrole carbon's resonance (130.9 ppm) is broader ($\nu_{1/2}$ = 800–1000 Hz) than that of **5** ($\nu_{1/2}$ = 250 Hz) due to the overlapping of three nonequivalent ^{13}C α-pyrrolic signals.

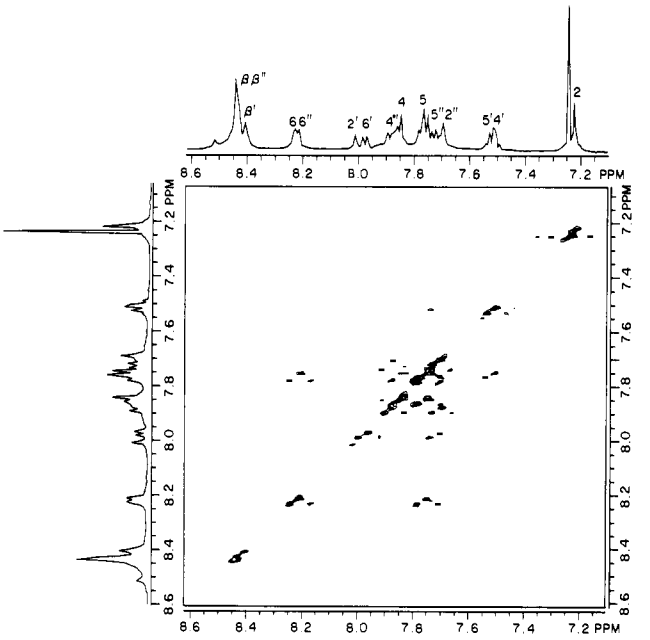

Figure 2. 2D ^1H–^1H correlation NMR spectrum of **9** in $CDCl_3$.

Porphyrin Dimer 10. The IR spectrum shows absorbances at 3360 (m), 3190 (w), 1660 (m), and 1560 (m) cm^{-1} corresponding to N—H of $H_2NC(O)$, pyrrolic N—H, C=O, and C=C, respectively. FABMS shows a base peak at 1565 corresponding to M^+. The pyrrolic N–H in ^1H NMR appears at −4.35 ppm, the benzylic protons at 4.38 ppm, two NHC(O) resonances at 6.61 and 6.95 ppm, the β-pyrrolic protons at 8.25 ppm, and the phenylic protons in the region of 7.58–7.95 ppm.

Physical Properties of Dimers Compared to Monomers. The absorption spectra of dimers **4–11** show Soret bands that are broadened (w = 16–21 nm in the dimers vs 12 nm in the monomers) and blue shifted (3–5 nm) compared to that of monomeric porphyrins such as **2** and **13** (see Table II). This is clearly the result of exciton coupling which has been shown to become important when two porphyrin moieties are brought together into

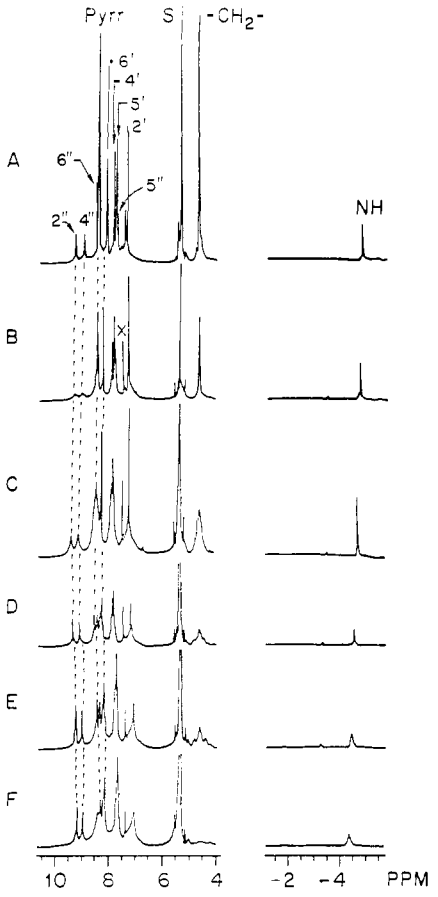

Figure 3. 500-MHz ^{1}H-NMR spectra of **5** in CD_2Cl_2 obtained at different temperatures. A, 25 °C; B, 0 °C; C, −20 °C; D, −40 °C; E, −60 °C; F, −80 °C. Labeling follows that in structure **5**, where Pyrr denotes the pyrrole, S residual undeuterated solvent, and X impurities in the solvent.

cofacial proximity.[14,21] Similarly, the fluorescence spectra of dimers **4–11** are significantly quenched by the chromophore–chromophore interactions in the dimer, and the magnitude of the quenching is determined by the interplanar distance of the two porphyrin cores (see Table III and Table I in the following paper in this issue). The ^{1}H NMR spectra of dimers **4–11** display resonances that are significantly upfield shifted compared to those of the corresponding monomeric porphyrins **2** and **13** (see Table I in the following paper in this issue).

Temperature Dependence of the ^{1}H NMR Spectra of the Dimers. The spectral changes produced upon cooling a methylene-d_2 chloride solution of a representative dimer, dimer **5**, are shown in Figure 3. Trace A of Figure 3 shows the spectrum of **5** at 25 °C where the resonances have been completely assigned. The signal at 8.1 ppm is due to the β-pyrrolic protons, while the signals at 8.9 and 9.1 ppm are due to the 2″ and 4″ protons of the pyridine in the pyridinesulfonamide groups. Examination of Figure 3 shows that upon cooling the sample to −80 °C the β-pyrrolic resonance undergoes the following changes. Between 0 and −20 °C, the β-pyrrole resonance broadens until at −60 °C two distinct signals are observed. Further, cooling of the sample shows an assymmetric broadening of the two pyrrole resonances. Similarly, the resonances corresponding to the 2″ and 4″ protons of the pyridine in the pyridinesulfonamide group also undergo broadening between 0 and −20 °C, but they sharpen dramatically upon further decrease in temperature. We ascribe these changes in the β-pyrrole and 2″ and 4″ proton resonances in the 0 to −60 °C region to the "freezing-out" of the two N–H tautomers in the porphyrins where the low field signal corresponds to the pyrrole ring carrying the protonated nitrogen.[22] As would be expected, the N–H resonance (−4.3 ppm) in this temperature range is unaffected and remains a singlet. Upon cooling the sample to −80 °C (trace F), the spectrum shows the splitting of the N–H resonance into two resonances of unequal intensity and an assymmetric broadening of the β-pyrrole resonances. We ascribe these observations to "freezing-out" more than one conformation of **5**, which undergo a relatively slow exchange on the NMR time scale.

Effect of DMSO on the Conformations of the Dimers. CHARM$_m$ molecular mechanics calculations in the gas phase predict symmetrical conformations for dimers **5**, **7**, **8**, **10**, and **11**. This suggests that in the absence of strong interaction between the solvent and the porphyrin, these dimers will exist in one symmetrical conformation in solution. Examination of the ^{1}H NMR of the tetracationic porphyrin dimer **7** revealed that at room temperature this dimer exists in more than one conformation in DMSO. Since **7** is not soluble in an inert solvent, comparison of its spectrum in DMSO to that in the inert solvent is not feasible. In order to better understand the nature and the modes of the effect of DMSO on the conformation of the dimer, spectral properties of similar dimers were investigated in $CHCl_3$ (an inert solvent) and DMSO. Examination of Tables II and III indicates that the absorption and emission spectra of dimers **5** and **11** are dramatically affected by the nature of the solvent, whereas those of dimers **8** and **9** and monomers **2** and **13** are quite unchanged. The Soret bands of **5** and **11** are broadened and blue shifted and their visible absorptions are significantly red shifted in DMSO compared to that in chloroform (see Table II). Similarly, the ^{1}H NMR spectral data of **5** and **11** in DMSO-d_6 show four pyrrolic N–H resonances in the region of −5.2 to −6.1 ppm, which indicates that those dimers exist in more than one conformation. On the other hand, their ^{1}H NMR spectral data in $CDCl_3$ show only one pyrrolic N–H resonance in the region of −4.3 to −4.4, which suggests the existence of only one conformation. In contrast, the ^{1}H NMR spectral data of dimers **8** and **9** and monomers **2** and **13** are not changed on switching from $CDCl_3$ to DMSO-d_6. The conformational changes on transfer from chloroform to DMSO with the dimeric porphyrins **5** and **11** can also be observed from their fluorescence spectra (Table III). The two emission bands of **5** and **11** in DMSO are red shifted (4.3–5.3 nm) and their intensities are decreased or unchanged compared to that in $CHCl_3$ (intensity ratio DMSO/$CHCl_3$ for the band at 650 nm is 0.815–1.069, and for the band at 712 nm is 0.667–0.866), whereas the emission spectra of the monomeric porphyrin **13** and the dimeric porphyrins **8** and **9** in DMSO are blue shifted or unchanged (−2.4 to 0 nm) and their intensities are higher than those in $CHCl_3$ (intensity ratio DMSO/$CHCl_3$ for the band at 650 nm is 1.355–1.954, and for the band at 712 nm is 1.125–1.60). The increase in the emission band intensities on transfer from chloroform to DMSO is a result of general solvent effects[23] which are strongly determined by the dielectric constant of the solvent. The decrease in the emission band intensities of DMSO solutions of dimers **5** and **11** compared to that of monomeric porphyrin **13** and dimeric porphyrins **8** and **9** is probably due to specific interactions between DMSO and the fluorophores of the dimers. Absorption and ^{1}H NMR spectra of dimers **5** and **11** were recorded in the concentration range from 1×10^{-2} to 5×10^{-6} M, and it was found that all the dimers exhibit unchanged spectral features regardless of the concentration. This indicates that interactions between DMSO and the dimers is not a result of aggregation and the source of the effect seen is a result of interactions between DMSO and the two porphyrin cores in the dimer. We find that metalation by $ZnCl_2$ or protonation by trifluoroacetic acid inhibits the interaction between DMSO and the dimer, and as a result, the corresponding biszinc and tetraprotonated porphyrin dimers exhibit only one conformation in DMSO. ^{1}H NMR variable-temperature experiments of **5** in DMSO show the conformation of **5** to be greatly affected by

(21) (a) Chang, C. K. *J. Heterocycl. Chem.* **1977**, *14*, 1285. (b) Collman, J. P.; Elliott, C. M.; Halbert, T. R.; Tovong, B. S. *Proc. Natl. Acad. Sci. U.S.A.* **1977**, *74*, 18.

(22) Storm, C. B.; Teklu, Y. *J. Am. Chem. Soc.* **1972**, *94*, 1745.

(23) Lakowicz, J. R. *Principles of Fluorescence Spectroscopy*; Plenum Press: New York, 1983; Chapter 7.

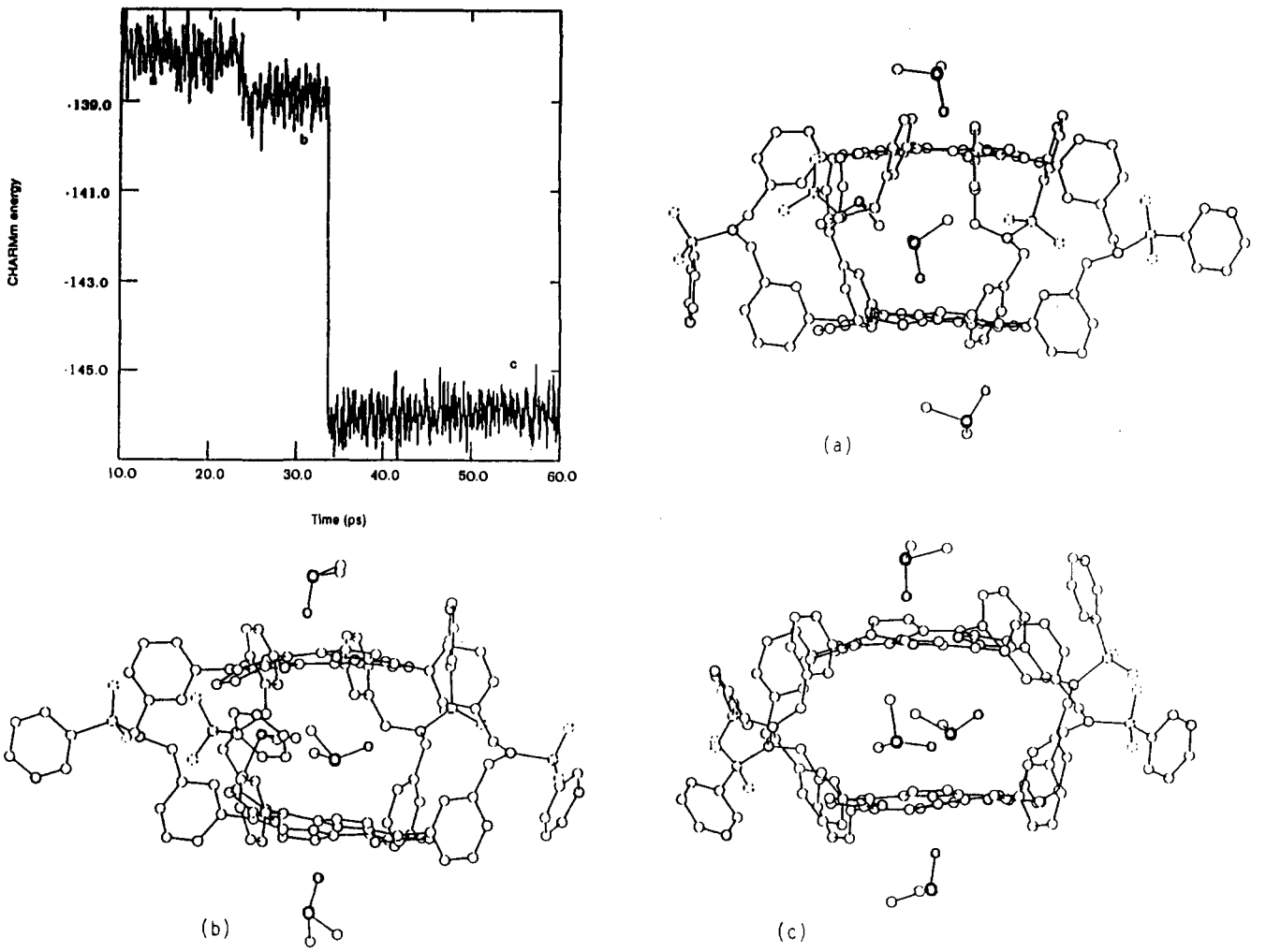

Figure 4. Top left: Dynamics trajectory for dimer **5**, collection phase in case ii (see text). (a) Structure at 11 ps, (b) structure at 30 ps, and (c) structure at 56 ps.

temperature. While at room temperature the ^{1}H NMR spectrum of **5** shows four pyrrolic N–H resonances in the region of −4.5 to −5.5 ppm, more than eight benzylic resonances in the region of 4.6–5.7 ppm and a complex aromatic region at 7.0–9.6 ppm, at 150 °C the four pyrrolic N–H resonances coalesced to give only one resonance at −5.4 ppm and the complex benzylic region coalesced to furnish one broad resonance at 4.9 ppm. This indicates that at room temperature **5** exists in more than one conformation and at higher temperatures (150 °C) only one conformation is populated. It would appear that a hydrogen bonding or van der Waals network exists between DMSO and **5** which results in more than one conformation. This is destroyed, upon heating to 150 °C, to furnish an average conformation.

Theoretical Calculations. In order to better understand the nature of the interactions between DMSO and dimers **5**, **7**, and **11**, CHARM$_m$ calculations of **5** "solvated" with DMSO were performed.[24] The DMSO solvation was conducted by placing four DMSO molecules in proximity to the four pyrrolic N–H protons of the two porphyrin cores. The vacuum global minimum structure was used as a starting geometry. Two kinds of calculations were done: (i) one where all DMSO molecules are outside the porphyrin cavity, two on each open porphyrin face, and (ii) one where two DMSO entities are placed inside the cavity and the other two are placed each on one open porphyrin face. Distances from DMSO oxygen to the protons of the porphyrin N–H were selected to be 2.3 Å. The hydrogen-bonding facility in CHARM$_m$ was activated, and initially a light constraint was placed on these distances. After 100 steps of steepest descents minimization, the constraints were removed and an additional 2000 steps in the adopted basis Newton–Raphson algorithm were performed. Finally, 60-ps dynamics runs were performed on the minimized structures at 300 K. The calculated global minimum structure of **5** in case i shows that only two DMSO molecules engage in hydrogen bonding with the two pyrrolic NH protons on each face of the two porphyrin cores, while the other two are moved away. The dynamics trajectories for this arrangement were unremarkable. The energy of solvated **5** was mostly constant over the 50-ps collection phase (see Experimental Section), and the starting geometry was largely retained. The hydrogen-bonding and van der Waals terms as calculated by CHARM$_m$ for **5** are −9.7 and 4.1 kcal/mol, respectively. The CHARM$_m$ total energy calculated for this arrangement is 131.7 kcal/mol (see Table IV).

In the calculation in case ii, the dynamics trajectory for **5** over the 50-ps collection phase showed three different plateaus corresponding roughly to three discrete conformations (see Figure 4). The first plateau corresponds to a conformation where one of the two DMSO molecules located in the cavity and one of the

Table IV. Energies[a] from Dynamics Simulation of Dimer **5** Interacting with DMSO

structure	E_{VDW}[d]	E_{HB}[e]	E_{TOTAL}[f]
i[b]	4.1	−9.7	131.7
ii a[c]	−3.0	−9.7	132.6
ii b[c]	−3.2	−9.7	130.2
ii c[c]	−4.2	−9.7	125.8

[a] Energies are in units of kcal/mol. [b] Global minimum conformation in case i (see text for definition). [c] See Figure 4. [d] E_{VDW} is the van der Waals energy. [e] E_{HB} is the hydrogen-bonding energy. [f] E_{TOTAL} is the total energy.

(24) Brooks, B. R.; Bruccoleri, R. E.; Olafson, B. D.; States, D. J.; Swaminathan, S.; Karplus, M. *J. Comput. Chem.* **1983**, *4*, 187.

two outside engage in a hydrogen-bonding arrangement with pyrrolic N–H each in a separate porphyrin ring (see a in Figure 4). Evidently, hydrogen bonding can take place inside the cavity, and the total energy of the system, 132.6 kcal/mol, is similar to that calculated in case i (see Table IV). After 23 ps, a slight lowering of energy affords a structure where both hydrogen bonds involve DMSO molecules located on the outside. The DMSO molecules inside are engaged in nonbonded interactions with the porphyrin moiety. One is situated near the center of the cavity, while the other progresses toward the periphery (see b in Figure 4). The global minimum structure observed after 34 ps in which two DMSO molecules outside the porphyrin dimer form hydrogen bonds with the two pyrrolic NH's and one DMSO inside has moved to the outside, while the other has optimized its arrangement with respect to the two porphyrin planes (see c in Figure 4). The energy difference between the highest and the lowest energy conformers is roughly 8 kcal/mol, and the calculated total energy of the global minimum is 125.8 kcal/mol (see Table IV). In all structures, the factor that changes the most is the van der Waals energy of the system, which appears to be minimized when a DMSO is cushioned between the two porphyrin planes. The hydrogen-bonding and van der Waals terms calculated by $CHARM_m$ for **5** in case ii are −9.7 and −4.2 kcal/mol, respectively (see Table IV). Inspection of the structures in Figure 4 indicates that the conformations are less symmetrical than the calculated vacuum global minimum structure. Calculations of the cyano dimer **8** were carried out in the same manner. Cases i and ii both afforded symmetrical structures with DMSO, since the cavity of the starting structure (p–p = 5.75 Å; see Table I in the following paper in this issue) is larger than that of **5** (p–p = 5.0 Å; see Table I in the following paper in this issue) and no cnoformational change needs to take place to accommodate DMSO molecules inside. The combined results strongly suggest that interactions of **5** with DMSO are more important in case ii than in case i and speaks for marked intracavity interactions with DMSO in this dimer which result in discrete, unsymmetrical conformations.

Summary

Several novel water- and non-water-soluble symmetrical and unsymmetrical quadruply aza bridged closely interspaced cofacial bis(5,10,15,20-tetraphenylporphyrin)s and the corresponding biszinc complexes have been synthesized and fully characterized by 1D and 2D NMR methods, as well as by other spectral techniques. As expected,[14,21] UV/vis, fluorescence, and ^1H NMR spectra of the porphyrin dimers display characteristics quite different from monomeric porphyrins and they indicate that the two porphyrin cores in the dimer are cofacial and in close proximity to enable the existence of $\pi-\pi$ interactions between them. ^1H NMR spectra of porphyrin dimers **5**, **7**, and **11** in DMSO-d_6 at room temperature indicate the existence of a strong interaction between the dimers and DMSO which results in more than one conformation. This is supported by the $CHARM_m$ molecular dynamics calculations of the DMSO-solvated dimer **5** which show that the symmetrical conformation of **5** observed in the gas-phase computer simulations is perturbed and at least three energetically different conformations are obtained as a result of intracavity interactions between DMSO and the dimer. The ^1H NMR of the DMSO-d_6 solution of **5** recorded at 150 °C indicates the presence of only one conformation, indicating that weeak forces were responsible for the presence of the three different conformations at room temperature.

Experimental Section

General. General nuclear magnetic resonance spectra were obtained on Nicolet NT-300 and General Electric GN-500 spectrophotometers at 25 °C. Chemical shifts (ppm) were referenced to $CHCl_3$ (^1H, 7.240 ppm; ^{13}C, 77.000 ppm). Phase-sensitive double-quantum-filtered COSY spectra were recorded using the pulse sequence[25] $90°-t_1-90°_{\phi 1}-\Delta-90°_{\phi 2}$–aquisition$_{\phi R}$ with a 90° pulse of 22.5 μs calibrated before the experiment, Δ = 8 μs, and an eight-step phase cycling has been applied.[26,27] Spectra were collected into 4K data blocks for 256 t_1 increments with a relaxation delay of 1.5 s. The spectral width in both dimensions was 7092.19 Hz for **5** and 8333.33 Hz for **9**. The data matrix was zero filled to 2K and apodized with an exponential function to give a line broadening of 1 Hz in both dimensions. Two-dimensional (2D) $^{13}C-^1H$ heteronuclear shift correlation data were recorded using the pulse sequences[28] (^1H) $90°_{\phi 1}-t_1-\Delta_1-90°_{\phi 2}-t-\Delta_2$–decouple and ($^{13}C$) $t_{1/2}-180°_{\phi 1}-t_{1/2}-\Delta_1-t-90°_{\phi 3}-\Delta_2$–aquisition$_{\phi R}$ with a 90° (^{13}C) pulse of 17.5 μs, with a 90° (^1H) pulse of 32 μs calibrated before the experiment, and with an eight-step phase cycling[28] to afford quadrature detection in both frequency domains. Spectra were collected into 4K data blocks for 130 t_1 increments with a relaxation delay of 1.5 s, Δ_1 = 3.2 ms, Δ_2 = 2.1 ms, and τ = 10 μs. The spectral width in the first dimension was 8333.33 Hz and 15 151.50 Hz in the second dimension. The data matrix was zero filled to 1K and apodized with a double-exponential function to give a line broadening of 3 Hz in both dimensions. Infrared spectra were determined on a Perkin-Elmer 1330 spectrophotometer. Absorption spectra were recorded on a Cary-14 spectrophotometer interfaced to a Zenith computer equipped with OLIS (On-Line Instrument System Inc.) data acquisition and processing software. Fast atom bombardment (FAB) mass spectroscopy was performed at UCSB using *m*-nitrobenzyl alcohol as the matrix and a parallel run of cesium rubidium iodide as the reference. Emission spectra were run on a Perkin-Elmer LS 50. Melting points were taken on a Laboratory Devices MEL-TEMP apparatus and are uncorrected. α-Bromo-*m*-tolunitrile, pyrrole, diisobutylaluminum hydride (DIBAL-H), methyl iodide, cyanamide, phosphorus oxychloride, phosphorus pentachloride, trifluoroacetic acid, ammonium hydroxide, cesium carbonate, and 3-pyridinesulfonic acid were purchased from Aldrich. All other reagents were commercially obtained in high purity. All reactions were carried out with purified reagents in dry, purified solvents under argon unless noted otherwise. Column chromatography was performed with Fischer Type 60-Å (200–425-mesh) silica gel. Preparative thin-layer chromatography (TLC) was performed by using E.M. Sciences Kieselgel 60 F_{254}. Reverse-phase preparative thin-layer chromatography was performed by using Whatman PLKC18F glass-backed plates.

Theoretical Calculations. All model building and calcultions were performed on a Silicon Graphics IRIS 4D/220 GTX workstation, using the programs Quanta version 3.2 (Polygen Corp.) and $CHARM_m$[24] version 21.2. The topology file PORPHYRINH.RTF supplied by Polygen was used as a basis for the porphyrin moieties. DMSO was constructed in Chemnote and geometry optimized by using the AM1 semiempirical method[29] interfaced to Quanta. Solvent molecules were placed interactively in a 3D molecular modeling mode. The sulfoxide oxygen was defined as a hydrogen-bonding donor in the corresponding RTF file generated, and the appropriate donors and acceptors were likewise defined for the dimers. Atom constraints to 2.3-Å separation were imposed on the atoms involved in hydrogen bonding for the first 100 steps of steepest descent minimization. Constraints were removed, and further minimization with the adopted basis Newton–Raphson algorithm was performed. Molecular dynamics to 60 ps at 300 K were calculated, with a 3-ps heating phase, 7-ps equilibration phase, and finally a 50-ps collection phase. Analysis of the final 50 ps was performed by using dynamics animation and search facilities in Quanta.

α-Bromo-*m*-tolualdehyde (1). The earlier preparation of **1** was modified in the following manner.[14,15] A solution of 1 M diisobutylaluminum hydride (DIBAL-H) in heptane (105 mL) was added in a dropwise manner over a period of 10 min to a solution of α-bromo-*m*-tolunitrile (17 g, 86.7 mmol) in dry benzene (170 mL) at 10 °C. The resulting solution was stirred at room temperature for 1.5 h and then diluted with THF (50 mL) and cooled down to 0 °C. A 10% aqueous HCl solution (30 mL) was added in a dropwise manner to avoid overheating, and the resulting mixture was stirred at room temperature for 1 h. The layers were separated, and the aqueous layer was extracted with ether (3×). The combined organic layer was washed with water and brine, dried over anhydrous $MgSO_4$, filtered, and evaporated to give a white solid which was recrystallized from ether/hexane to yield 14.3 g (84%) of aldehyde **2**:[14,15] mp 45–46 °C; IR (KBr) 1595, 1610 (m, C=C), 1710 (s, C=O); ^1H NMR ($CDCl_3$) δ 4.54 (s, 2 H, CH_2Br), 7.51 (t, 1 H, *J* = 8 Hz), 7.66 (d, 1 H, *J* = 8 Hz), 7.82 (dt, 1 H, *J* = 8.1 Hz), 7.90 (s, 1 H), 10.02 (s, 1 H, CHO); ^{13}C NMR ($CDCl_3$) δ 32.0 (CH_2Br), 129.6, 129.7, 129.8, 134.8, 136.8, 138.9, 191.6 (CHO).

5,10,15,20-Tetrakis(α-bromo-*m*-tolyl)porphyrin (2). The earlier preparation of porphyrin **2**[14] was modified in the following manner.

(25) Martin, G. E.; Zekter, A. S. *Two Dimensional NMR Methods for Establishing Molecular Connectivity*; VCH: New York, 1988; p 100.

(26) Wokaun, A.; Ernst, R. R. *Chem. Phys. Lett.* **1977**, *52*, 407.
(27) Morris, G. A. *Magn. Reson. Chem.* **1980**, *24*, 371.
(28) See ref 25, p 178.
(29) Dewar, M. J. S.; Zoebisch, E. G.; Healy, E. F.; Stewart, J. J. P. *J. Am. Chem. Soc.* **1985**, *107*, 3902.

Boron trifluoride etherate (1.23 mL, 10 mmol) was added to a solution containing aldehyde **1** (5.96 g, 30 mmol) and dry pyrrole (2.08 mL, 30 mmol) in dry chloroform (2.8 L). The reaction mixture was stirred at room temperature for 1.5 h. Triethylamine (1.7 mL, 12 mmol) and then tetrachloro-1,4-benzoquinone (5.54 g, 22.6 mmol) were added, and the resulting solution was heated at 60 °C for 30 min. The reaction mixture was evaporated, and the resulting purple solid was trituated with ether, filtered, and evaporated. The resulting residue was dissolved in a minimum amount of chloroform and was subjected to flash chromatography using silica gel and eluting with a mixture of ethyl acetate/hexanes (3:10) to give 1.8 g (24.4%) of **2** as a purple solid:[14] IR ($CHCl_3$) 3325 (w, NH), 1605, 1590, 1570 (m, C=C); ^1H NMR ($CDCl_3$) δ −2.80 (s, 2 H, NH), 4.76 (s, 8 H, CH_2Br), 7.73 (t, 4 H, J = 7.5 Hz, H-5′), 7.81 (d, 4 H, J = 7.5 Hz, H-6′), 8.14 (d, 4 H, J = 7.5 Hz, H-4′), 8.25 (s, 4 H, H-2′), 8.86 (s, 8 H, β-pyrrolic H); ^{13}C NMR ($CDCl_3$) δ 33.5 (CH_2Br), 119.5 (meso), 127.2, 128.4, 131.3, 143.5, 135.0, 136.4, 142.5; FABMS m/z 982 (calcd for $C_{48}H_{34}Br_4N_4$ [M^+] m/z 981.9); UV/vis ($CHCl_3$) λ_{max} ($\epsilon \times 10^{-3}$ cm^{-1} M^{-1}) 419 (324), 515 (16.1), 549 (7.2), 589 (5.5), 646 (3.4).

3-Pyridinesulfonyl Chloride (3). A mixture of 3-pyridinesulfonic acid (15 g, 94.3 mmol) and phosphorus pentachloride (24 g, 115.4 mmol) in phosphorus oxychloride (30 mL) was heated at 120 °C for 12 h. The reaction mixture was cooled to room temperature and diluted with dry chloroform (100 mL). The resulting suspension was saturated with HCl gas, and the white precipitate obtained was immediately collected, washed with dry chloroform, and dried at 25 °C/0.2 mmHg to give 19.7 g (98%) of **3** as a white solid: mp 138–140 °C (lit.[17] mp 141–144 °C); IR (Nujol) 1625 (m, C=C), 1590 (m, C=N), 1180–1190, 1100 (s, SO_2); ^1H NMR (DMSO-d_6) δ 8.07 (t, 1 H, J = 8 Hz, H-5″), 8.67 (d, 1 H, J = 8 Hz, H-6″), 8.88 (s, 1 H, NH), 9.08 (d, 1 H, J = 6 Hz, H-4″), 9.16 (s, 1 H, H-2″); ^{13}C NMR (DMSO-d_6) δ 128.2, 138.7, 142.5, 143.2, 147.0.

3-Pyridinesulfonamide (4). A mixture of 3-pyridinesulfonyl chloride (6.42 g, 30 mmol) in 28% aqueous ammonium hydroxide solution (100 mL) was heated at 50 °C for 2 h, cooled, and evaporated to dryness. The resulting solid residue was triturated with dry acetone (100 mL) and filtered. The filtrate was dried over anhydrous $MgSO_4$, filtered, and evaporated to yield a yellow solid which was recrystallized from acetone/chloroform to yield 3.14 g (66%) of **4** as a yellow solid: mp 108–110 °C (lit.[18] mp 110–111 °C); IR (KBr) 3320 (m, NH), 1590 (m, C=C), 1570 (w, C=N), 1180, 1120 (s, SO_2); ^1H NMR (DMSO-d_6) δ 7.56 (br s, 2 H, NH), 7.62 (dt, 1 H, J = 7.3 Hz), 8.18 (dd, 1 H, J = 8.2 Hz), 8.78 (dd, 1 H, J = 6.1 Hz), 8.97 (d, 1 H, J = 2.5 Hz); ^{13}C NMR (acetone-d_6) δ 123.4, 133.4, 146.3, 146.7, 152.0; FABMS m/z 159 (calcd for $C_5H_6N_2O_2S$ [M + 1] m/z 159).

Tetrakis[*m*,*m*-(methylene(*m*-pyridinesulfonyl)imino)methylene]-strati-bis(5,10,15,20-tetraphenylporphyrin) (5) and Its Biszinc Complex (Zn_2-5). Preparation of 5. Cesium carbonate (938 mg, 2.88 mmol) was added to a solution containing **2** (474 mg, 0.48 mmol) and **4** (152 mg, 0.96 mmol) in dry DMF (500 mL). The reaction mixture was stirred at room temperature overnight and then evaporated to dryness. The purple solid obtained was dissolved in chloroform (50 mL), filtered, and evaporated. The resulting purple residue was subjected to flash chromatography using silica gel and eluting with a mixture of chloroform/methanol (100:3). The nonpolar purple bands were collected, the residue obtained was divided into four fractions, and each fraction was subjected to preparative TLC on a 0.5 × 200 × 200 mm silica plate eluting with a mixture of chloroform/methanol (100:3). Two bands were collected and were treated with trifluoroacetic acid (1 mL). The resulting green solution of each of the bands was diluted with chloroform, washed with 5% aqueous ammonium hydroxide solution, water, and brine, dried over anhydrous Na_2SO_4, and evaporated to give a purple powder. The polar band gave 56 mg (12%) of **5** as a purple solid, and the nonpolar band gave 4.7 mg (1.2%) of **6** as a purple powder. IR ($CHCl_3$) 3320 (w, NH), 1600 (m, C=C), 1575 (w, C=N), 1160, 1110 (s, SO_2); ^1H NMR ($CDCl_3$) δ −4.34 (s, 4 H, NH), 4.69 (s, 16 H, CH_2), 7.06 (s, 8 H, H-2′), 7.56 (t, 8 H, J = 8.5 Hz, H-5″), 7.63 (t, 4 H, J = 7.5 Hz, H-5′), 7.76 (d, 8 H, J = 6.5 Hz, H-4′), 7.96 (d, 8 H, J = 6.5 Hz, H-6′), 8.16 (s, 16 H, β-pyrrolic H), 8.29 (d, 4 H, J = 8 Hz, H-6″), 8.89 (d, 4 H, J = 6 Hz, H-4″), 9.23 (s, 4 H, H-2″); ^{13}C NMR ($CDCl_3$) δ 49.5 (CH_2), 118.3 (meso), 123.67 (C-5″), 127.42, (C-5′), 128.58 (C-4′), 130.69 (β-pyrrolic), 132.57 (C-3′), 133.21 (C-6′), 134.90 (C-6″), 135.06 (C-2′), 137.98 (C-1″), 141.96 (C-1′), 143.3 (α-pyrrolic), 148.23 (C-2″), 153.17 (C-4″); FABMS m/z 1957 (calcd for $C_{116}H_{84}N_{16}O_8S_4$ [M^+] m/z 1956.6); UV/vis ($CHCl_3$) δ_{max} ($\epsilon \times 10^{-3}$ cm^{-1} M^{-1}) 406 (sh, 314), 414 (415), 514 (23.6), 550 (11.2), 591 (7.1), 647 (3.7); emission ($CHCl_3$) max, nm (rel intensity) 651.5 (20.7), 713.8 (11.08), 787.1 (4.43); (DMSO) 655.8 (10.1), 719.1 (1.0), 786.6 (1.9).

Preparation of Zn_2-5. A solution of **5** (10 mg, 0.0051 mmol) in chloroform (30 mL) was added to 10 mL of a methanolic solution containing 15 mg of potassium acetate (0.15 mmol) and 15 mg of $Zn(OAc)_2 \cdot 2H_2O$ (0.68 mmol). The reaction mixture was stirred at room temperature for 5 h and then diluted with chloroform (100 mL) and THF (150 mL). The reaction mixture was extracted with 5% aqueous ammonium hydroxide solution, water, and brine, and the organic layer was separated, dried over anhydrous Na_2SO_4, filtered, and evaporated to yield a pink powder. The resulting pink residue was subjected to preparative TLC on a 0.5 × 200 × 200 mm silica gel plate eluting with a mixture of $CHCl_3$/MeOH (50:3). The pink band was collected to yield 10 mg (94%) of Zn_2-**5** as a pink solid: FABMS m/z 2084 (calcd for $C_{116}H_{80}N_{16}O_8S_4Zn_2$ [M^+] m/z 2083.4); UV/vis (DMSO) λ_{max} ($\epsilon \times 10^{-3}$ cm^{-1} M^{-1}) 413 (sh, 160), 422 (377), 560 (17.0), 600 (5.2).

Tris[*m*,*m*-(methylene(*m*-pyridinesulfonyl)imino)methylene]-mono-((((methyleneoxy)carbonyl)oxy)methylene)-strati-bis(5,10,15,20-tetraphenylporphyrin) (6). **6** was prepared in the same manner as **5** by using cesium carbonate (938 mg, 2.88 mmol), **2** (474 mg, 0.48 mmol), and **4** (114 mg, 0.72 mmol) in dry DMF (500 mL). After workup and chromatographic separation (in the same manner described for **5**), 35 mg (7%) of **5** and 17 mg (3.4%) of **6** were obtained. IR (Nujol) 3200 (NH, w), 1740 (C=O, m), 1670 (C=N, m), 1600 (C=C, m); ^1H NMR ($CDCl_3$) δ −3.95 (s, 4 H, NH), 4.57 (s, 8 H, CH_2), 4.75 (s, 4 H, $CH_{2''}$), 5.42 (s, 4 H, $CH_{2'}$), 6.88 (s, 4 H, H_2), 7.42 (s, 2 H, $H_{2'}$), 7.45 (d, 2 H, J = 7 Hz, $H_{4'}$), 7.58 (t, 2 H, J = 7.5 Hz, $H_{5'}$), 7.60 (t, 6 H, J = 7 Hz, H_5, $H_{5''}$), 7.74 (d, 6 H, J = 7.5 Hz, H_4, $H_{4''}$), 780 (s, 2 H, $H_{2''}$), 8.09 (d, 2 H, J = 7 Hz, $H_{6'}$), 8.15 (d, 6 H, H_6, $H_{6''}$), 8.18 (s, 16 H, β-pyrrolic H), 8.20 (t, 3 H, $H_{5'''}$), 8.61 (d, 3 H, J = 6.5 Hz, $H_{6'''}$), 8.78 (dd, 3 H, J = 7, 7 Hz, $H_{4'''}$), 9.06 (d, 2 H, J = 2 Hz, $H_{2'''}$), 9.18 (d, 1 H, J = 2 Hz, $H_{2'''a}$); ^{13}C NMR ($CDCl_3$) δ 49.69 (CH_2 and $CH_{2''}$), 66.79 ($CH_{2'}$), 118.32, 118.48 (meso), 123.70, 123.6 ($C_{6'''}$ and $C_{6'''a}$), 127.86 ($C_{4'}$), 127.48 (C_5 and $C_{5''}$), 127.38 ($C_{5'}$), 128.37 (C_4 and $C_{4''}$), 130.55 (β-pyrrolic), 132.70, 133.06, 133.21 (C_6, $C_{6'}$ and $C_{6''}$), 134.91, 135.00 ($C_{5'''}$ and $C_{5'''a}$), 136.16, 136.30, 137.99 (C_2, $C_{2'}$, and $C_{2'''}$), 137.99, 138.05, 138.13 (C_1, $C_{1'}$, and $C_{1''}$), 142.03 (α-pyrrolic), 142.12, 142.27 ($C_{1'''}$ and $C_{1'''a}$), 148.19, 148.32 ($C_{2'''}$ and $C_{2'''a}$), 153.08, 153.21 ($C_{4'''}$ and $C_{4'''a}$), 171.96 (C=O); FABMS m/z 1860.6 (calcd for $C_{112}H_{80}N_{14}O_9S_3$ [M^+] m/z 1860.6); UV/vis ($CHCl_3$) λ_{max} ($\epsilon \times 10^{-3}$ cm^{-1} M^{-1}) 416 (744), 517 (28.8), 553 (14.0), 591 (11.5), 648 (6.7); emission ($CHCl_3$) max, nm (rel intensity) 650.6 (9.9), 713.3 (1.17), 787.5 (1.0); emission (DMSO) max, nm (rel intensity) 653.4 (19.3), 716.2 (1.86), 780.0 (1.0).

Tetrakis[*m*,*m*-(methylene(*m*-pyridiniumsulfonyl)imino)methylene]-strati-bis(5,10,15,20-tetraphenylporphyrin) Chloride (7) and Its Biszinc Complex (Zn_2-7). A mixture of **5** (74 mg, 0.038 mmol), methyl iodide (10 mL, 160.6 mmol), chloroform (10 mL), and acetone (10 mL) was refluxed overnight. The reaction mixture was evaporated to dryness, and the resulting purple solid residue was subjected to preparative reverse-phase TLC on a 1.0 × 200 × 200 mm Whatman PLKC18F plate eluting with a mixture of acetone/water/brine (90:9:1). The purple band was collected, and the residue obtained was passed through an ion-exchange column with resin in the chloride form (Dowex IX8-100/Cl^-) and eluting with a mixture of water/methanol. The purple solution was collected and evaporated to give 57 mg (70%) of **7** as a purple solid: ^1H NMR (CD_3COCD_3, 0.5% CF_3COOH) δ −4.3 (s, 4 H, NH), 4.98 (br s, 28 H, NCH_3 and CH_2Br), 7.10 (br s, 8 H, H-2′), 7.91 (br s, 8 H, H-5′), 8.02 (br s, 8 H, H-4′), 8.19 (br s, 8 H, H-6′), 8.25 (s, 16 H, β-pyrrolic H), 8.75 (br s, 4 H, H-5″), 9.40 (br s, 4 H, H-6″), 9.71 (br s, 4 H, H-4″), 10.11 (br s, 4 H, H-2″); FABMS m/z 2017 (calcd for $C_{120}H_{96}N_{16}O_8S_4$ [M^+] m/z 2016.6); UV/vis (DMSO) λ_{max} ($\epsilon \times 10^{-3}$ cm^{-1} M^{-1}) 409 (351), 519 (17.4), 556 (13.1), 598 (9.3), 658 (7.6); emission (DMSO) max, nm (rel intensity) 660.5 (11.22), 723.4 (1.0). For more assignable ^1H NMR resonances, see the ^1H NMR of the corresponding biszinc complex (Zn_2-7).

Preparation of Zn_2-7. A mixture of **7** (10 mg, 0.005 mmol) and $Zn(OAc)_2$ (50 mg, 0.27 mmol) in dry DMF (10 mL) was heated at 95 °C for 2 h. The reaction mixture was cooled down to room temperature and evaporated to give a pink solid which was washed with cold water and ether and dried at 25 °C/0.2 mmHg for 12 h to yield 10.4 mg (98%) of Zn_2-**7** as a pink solid: ^1H NMR (acetone-d_6) δ 4.94 (br s, 28 H, CH_2 and NCH_3), 7.35 (s, 8 H, H-2′), 7.78 (t, 8 H, J = 7 Hz, H-5′), 7.88 (d, 8 H, J = 7 Hz, H-4′), 8.10 (d, 8 H, J = 7 Hz, H-6′), 8.21 (s, 16 H, β-pyrrolic H), 8.73 (t, 4 H, J = 7 Hz, H-5″), 9.39 (d, 4 H, J = 7 Hz, H-6″), 9.55 (d, 4 H, J = 7 Hz, H-4″), 9.95 (s, 4 H, H-2″). In DMSO-d_6, the peak at 4.94 appears as two singlets: ^1H NMR δ 4.82 (s, 16 H, CH_2), 4.95 (s, 12 H, NCH_3); FABMS m/z 2139 (calcd for $C_{120}H_{92}N_{16}O_8S_4Zn_2$ [M^+] m/z 2140.5); UV/vis (DMSO) λ_{max} ($\epsilon \times 10^{-3}$ cm^{-1} M^{-1}) 413 (sh, 185), 421 (347), 559 (17.6), 598 (4.2).

Tetrakis[*m*,*m*-(methylenecyanoimino)methylene]-strati-bis-(5,10,15,20-tetraphenylporphyrin) (8). Following the procedure described previously,[14] using cesium carbonate (1.88 g, 5.6 mmol), **2** (948 mg, 0.96 mmol), and cyanamide (80.6 mg, 1.92 mmol) in dry DMF (960 mL) and chromatographic separation in the same manner described, porphyrins **8** and **9** were obtained in 5% and 1% yields, respectively. IR ($CHCl_3$)

3320 (NH, w), 2230 (CN, s), 1600, 1580 (C=C, m); ^{1}H NMR ($CDCl_3$) δ −3.99 (s, 4 H, NH), 4.44 (s, 16 H, CH_2), 7.32 (s, 8 H, H-2′), 7.74 (t, 8 H, J = 8 Hz, H-5′), 7.84 (d, 8 H, J = 8 Hz, H-4′), 8.14 (d, 8 H, J = 8 Hz, H-6′), 8.38 (s, 16 H, β-pyrrolic H); ^{13}C NMR ($CDCl_3$) δ 54.36 (CH_2), 118.22 (CN), 118.6 (meso), 127.45 (C-5′), 128.43 (C-4′), 130.8 (β-pyrrolic), 132.34 (C-3′), 133.79 (C-6′), 134.57 (C-2′), 142.43 (C-1′), 149.19 (α-pyrrolic); FABMS m/z 1493 (calcd for $C_{100}H_{68}N_{16}$ [M$^+$] m/z 1492.6); UV/vis ($CHCl_3$) λ_{max} ($\epsilon \times 10^{-3}$ cm^{-1} M^{-1}) 415 (454), 514 (20.5), 550 (9.87), 591 (7.53), 649 (5.67); emission ($CHCl_3$) max, nm (rel intensity) 650.1 (14.19), 711.9 (1.64), 785.6 (1.0); emission (DMSO) max, nm (rel intensity) 649.6 (15.2), 712.4 (1.46), 787.1 (1.0).

Tris[*m*,*m*-(methylenecyanoimino)methylene]-mono((((methyleneoxy)carbonyl)oxy)methylene)-strati-bis(5,10,15,20-tetraphenylporphyrin) (9). Following the procedure described previously,[14] using cesium carbonate (940 mg, 2.8 mmol), **2** (474 mg, 0.48 mmol), and cyanamide (30.2 mg, 0.72 mmol) in dry DMF (500 mL) and chromatographic separation in the same manner described, porphyrins **8** and **9** were obtained in 4% and 3% yields, respectively. IR (Nujol) 3200 (NH, w), 2210 (CN, m), 1730 (C=O, m), 1600 (C=C, m); ^{1}H NMR ($CDCl_3$) δ −3.75 (s, 4 H, NH), 4.33 (s, 8 H, CH_2), 4.51 (s, 4 H, $CH_{2''}$), 5.50 (s, 4 H, $CH_{2'}$), 7.22 (s, 4 H, H_2), 7.49 (d, 2 H, J = 7.5 Hz, $H_{4'}$), 7.52 (t, 2 H, J = 7.5 Hz, $H_{5'}$), 7.69 (s, 2 H, $H_{2''}$), 7.71 (t, 2 H, J = 7.5 Hz, $H_{5''}$), 7.76 (t, 4 H, J = 7.5 Hz, H_5), 7.85 (d, 4 H, J = 7.5 Hz, H_4), 7.88 (d, 2 H, J = 8.0 Hz, $H_{4''}$), 7.97 (d, 2 H, J = 7.0 Hz, $H_{6'}$), 8.01 (s, 2 H, $H_{2'}$), 8.22 (d, 6 H, J = 7.0 Hz, H_6, $H_{6''}$), 8.40 (s, 4 H, β'-pyrrolic), 8.43 (s, 4 H, β- and β''-pyrrolic); ^{13}C NMR ($CDCl_3$) δ 54.10 (CH_2), 54.19 ($CH_{2''}$), 68.88 ($CH_{2'}$), 118.20 (CN), 118.51 (meso), 119.40 (CN″), 125.51 (C-5′), 126.28 (C-4′), 127.52 (C-5, and C-5″), 128.45 (C-4, C-4″), 130.86 (β-pyrrolic), 131.46 (C-3′), 132.45 (C-3″, C-3), 133.40 (C-6′), 133.75 (C-6″, C-6), 134.24 (C-2′), 134.44 (C-2), 134.57 (C-2″), 142.16 (C-1′), 142.40 (C-1, C-1″), 149.34 (α-pyrrolic); UV/vis ($CHCl_3$) λ_{max} ($\epsilon \times 10^{-3}$ cm^{-1} M^{-1}) 416 (718), 516 (30.0), 551 (17.8), 593 (6.9), 649 (4.7); FABMS m/z 1513 (calcd for $C_{100}H_{68}N_{14}O_3$ [M$^+$] m/z 1512.6); emission ($CHCl_3$) max, nm (rel intensity) 649.1 (8.81), 712.8 (1.0), 787.5 (1.37); emission (DMSO) max, nm (rel intensity) 649.1 (13.64), 712.8 (1.29), 788.0 (1.0).

Tetrakis[*m*,*m*-(methylene(formamido)imino)methylene]-strati-bis-(5,10,15,20-tetraphenylporphyrin) (10). A mixture of **8** (15 mg, 0.01 mmol) and trifluoroacetic acid (2.0 mL, 26 mmol) in ethanol (5 mL) was refluxed for 72 h. The reaction mixture was cooled to room temperature and diluted with methanol (50 mL), DMF (50 mL), and chloroform (100 mL). A 5% aqueous ammonium hydroxide solution (300 mL) was added, and the reaction mixture was stirred at room temperature for 15 min. The two layers were separated, and the organic layer was washed with water and brine, dried over anhydrous Na_2SO_4, and evaporated to yield a purple powder. The resulting purple residue was subjected to flash chromatography using silica gel and eluting with a mixture of chloroform/methanol (3:1). The purple band was collected to give 12 mg (76%) of **10** as a purple powder: IR (Nujol) 3360 (NH, br), 3190 (NH, w), 1660 (C=O, br s), 1560 (C=C, m); ^{1}H NMR (DMSO-d_6) δ −4.35 (s, 4 H, pyrrolic NH), 4.38 (s, 16 H, NCH_2), 6.61 (s, 4 H, C(O)NH), 6.95 (s, 4 H, C(O)NH), 7.58 (s, 8 H, H-2′), 7.65 (t, 8 H, J = 8 Hz, H-5′), 7.75 (d, 8 H, J = 8 Hz, H-6′), 7.95 (d, 8 H, J = 7 Hz, H-4′), 8.25 (s, 16 H, β-pyrrolic H); FABMS m/z 1565 (calcd for $C_{100}H_{76}N_{16}O_4$ (M$^+$) m/z 1564.6); UV/vis (DMSO) λ_{max} ($\epsilon \times 10^{-3}$ cm^{-1} M^{-1}) 416 (517), 516 (21.8), 552 (8.1), 593 (6.9), 649 (4.7).

Acknowledgment. This study was supported by grants from the National Institute of health and Protos Corporation of Emeryville CA.

Registry No. 1, 82072-23-9; **2**, 133671-91-7; **3**, 16133-25-8; 4, 2922-45-4; **5**, 134260-60-9; Zn_2-**5**, 134286-04-7; **6**, 138312-91-1; **7**, 134209-10-2; Zn_2-**7**, 134286-03-6; **8**, 133672-00-1; **9**, 138312-92-2; **10**, 138312-89-7; **11**, 133671-99-5; **13**, 64397-83-7; α-bromo-*m*-tolunitrile, 28188-41-2; pyrrole, 109-97-7; 3-pyridinesulfonic acid, 636-72-6; cyanamide, 420-04-2.

Supplementary Material Available: ^{1}H and ^{13}C NMR spectra of compounds **5**–**10** and 2D ^{1}H–^{1}H spectrum of compound **9** (23 pages). Ordering information is given on any current masthead page.